



# Spatio-Temporal Agricultural Drought Monitoring Using Remote Sensing Indices

# 4

Syed Sadath Ali , Koyel Mukherjee ,  
Papia Kundu, and Piu Saha 

## Abstract

Drought is an intricate weather phenomenon; it directly affects food security and agricultural productivity. Accurate prediction of agricultural drought helps to take mitigation steps for reducing production losses. In the present study, agricultural drought was assessed by using the Normalized Difference Vegetation Index (NDVI), Vegetation Condition Index (VCI), Temperature Condition Index (TCI), and Vegetation Health Index (VHI) based on Landsat 8 and 9 data from 2013–2022. The LULC maps were also prepared using the supervised classification based on the maximum likelihood algorithm by the semi-automatic classification plugin (SCP) in QGIS from Sentinel-2 images. The remote sensing indices were calculated using a raster

calculator in ArcGIS software. The results of VCI indicate that 2014 and 2017 years were highly affected by drought, whereas 2016 was the most vulnerable year according to TCI. In 2017, the entire district was badly affected by VCI and TCI. The VHI results showed that 2015, 2016, and 2018 were the most drought-prone years. The spatial agricultural drought result shows that Chattna, Bankura I, Onda, and Ranibudh were extreme drought-affected blocks. Drought greatly impacts agriculture, so satellite-based drought data would benefit the understanding of the drought of Bankura district risk within the entire geographical area.

## Keywords

Agricultural drought · Temperature Condition Index · Vegetation Condition Index · Vegetation Health Index · Bankura

S. S. Ali  
Civil Engineering Department, Ballari Institute of  
Technology and Management, Ballari, Karnataka,  
India

K. Mukherjee  
Department of Geography, Rampurhat College, PO.  
Rampurhat, Dist. Birbhum, Rampurhat, West Bengal  
731224, India

P. Kundu · P. Saha (✉)  
Department of Geography and Applied Geography,  
University of North Bengal, PO. North Bengal  
University, Dist. Darjeeling, Siliguri, West Bengal  
734013, India  
e-mail: [piusaha.nbu@gmail.com](mailto:piusaha.nbu@gmail.com)

## 4.1 Introduction

Drought is a recurrent natural hazard that adversely affects the ecosystem, livelihoods, cultivation, and livestock farming (Alam et al. 2023; Ayugi et al. 2022), causing huge economic loss throughout the world (Guo et al. 2021; Zeng et al. 2022). It grows very slowly in the beginning but later it affects a large area with its severity (Liu et al. 2021). Based on physical

aspects, drought is classified as a meteorological, hydrological, and agricultural drought, among which ‘agricultural drought’ is characterized by insufficient moisture in the soil for cultivation at a particular time (Basak et al. 2022; Das et al. 2020). The intensity of ‘agricultural drought’ changes with space and time, and it is more challenging than other kinds of drought because it adversely degrades a particular region’s agricultural activity. In India, especially in the western part of West Bengal, agricultural drought has a crucial effect on agricultural production and productivity by disturbing the balance between food supply and demand (Gidey et al. 2018). Between 1900 and 2020, a drought event in India had a significant impact on over 1.4 billion people, resulting in a threatening situation for water resources and food security. This event has revealed that agricultural drought affects more than 68% of India’s land area (Nath et al. 2017), largely due to the rising trend of mean temperature, geo-environmental conditions, and climate change.

Under this critical situation, appraisal of agricultural drought could be helpful by using different spatio-temporal data from different sources like vegetation, hydrology, meteorology, etc. The spatial and non-spatial datasets are used for drought risk assessment (Apurv and Cai 2021; Hoque et al. 2021a; Kim et al., 2021). Remote sensing techniques are used in spatial analysis to support all the procedures (Hoque et al. 2021b; Zeng et al. 2022). The most popular remote sensing-based vegetation indices, such as Normalized Difference Vegetation Index (NDVI), Temperature Condition Index (TCI), Vegetation Condition Index (VCI), and Vegetation Health Index (VHI) have been used for the drought monitoring system (Hadri et al. 2021; Kogan 1997). The VHI is the most helpful satellite index to monitor agricultural drought (Wang and Yu 2021; Zhang et al. 2013). The Vegetation Health Index correlates with crop yield, the problem of crop health, and crop growth (Alahacoon et al. 2021; Zhao et al. 2022).

NDVI is one of the most popular vegetation health indices that analyze activities like respiration, transpiration productivity, temperature

variability, etc. (Pei et al. 2018). For instance, Nejadrekabi et al. (2022) observed the moisture period using NDVI in the Khuzestan province. Vegetation growth in China from 1982 to 2010 was evaluated using NDVI (Peng & Gitelson 2011). Agricultural drought monitoring for three months was calculated using NDVI in Raya of northern Ethiopia (Gidey et al. 2018). This chapter states that VCI and TCI can be used to delineate the seasonal and inter-annual drought, while Sultana et al. (2021) assessed agricultural drought severity in the northwestern part of Bangladesh from 1990 to 2018 by applying TCI, VCI, and VHI. Zambrano et al. (2016) measured the agricultural drought in the cropland of the Biobio region in Chile from 2000 to 2015 by analyzing the temporal and spatial variation of vegetation conditions with stress due to scarcity of rainfall with VCI.

The novelty of this current endeavor is to identify and monitor agricultural drought in the Bankura district of West Bengal using remote sensing data. Evaluation of drought indices, calculation intensity, severity, and duration of drought are the prime concern of this chapter which helps make a proper plan for mitigation and irrigation practice in drought-vulnerable areas through establishing an integrated relationship among NDVI, LST, VCI, TCI, and VHI methods which provide a guideline for future drought.

---

## 4.2 Study Area

Bankura is the fourth largest district of West Bengal, located between 22°30’N to 23°30’N latitudes and 87°00’E to 87°30’E longitudes, having a 6,882 km<sup>2</sup> area. The total population of the Bankura district is 3,992,309 persons, and the population density is 523 persons/km<sup>2</sup> (Census 2011). Bankura is a connecting link between the plain of West Bengal and the Plateau of Chotanagpur. The Purulia district in the west surrounds it, Purba Bardhaman and Paschim Bardhaman districts in the north, Jhargram and Paschim Medinipur in the south, and the Hugli district in the southeast. Darakeswar, Damodar,

Kangsabati, Silabati, and Gandhewari rivers drain the district. Geomorphologically, the Bankura district is a part of the Chotanagpur plateau (Fig. 4.1). There are three types of topographical terrain; i.e., the western part is a hilly region characterized by large granite rock covered by natural vegetation, the central part is undulating and characterized by red lateritic, and the eastern part is an alluvial plain covered by loamy soil. Following the topographic terrain, land use pattern of this area is also changing from east to west, and the low-lying alluvial plain of the northeast is mainly used for paddy cultivation. The western surface is undulating and gradually rising, so most of the land is covered by jungle. Bankura is part of Rarh, and agriculture is the main economic activity of this concerned study area, but it is challenged by low water availability, climatic change, and reduced annual rainfall. In the last few years, drought incidents and intensity have been increasing (Bhunia et al. 2020; Das et al. 2013). The

changing patterns of annual rainfall and 80% rainfall received during four months result in poor moisture in subsoil, which becomes a threat to crops and seriously affects the yields in the study area. The farmers of this area face some socio-economic problems; they lose their job and are forced to migrate. In recent times, Bankura district has become a geographer's attraction due to excessive drought proneness and its relation with the economy, poverty, mitigation, and migration-related scenarios (Raha and Gayen 2020).

## 4.3 Database and Methods

### 4.3.1 Database

In the present study, remote sensing data has been utilized from authenticated sources, and therefore, various drought indices are displayed by ESRI ArcGIS (Version 10.4.1) software.

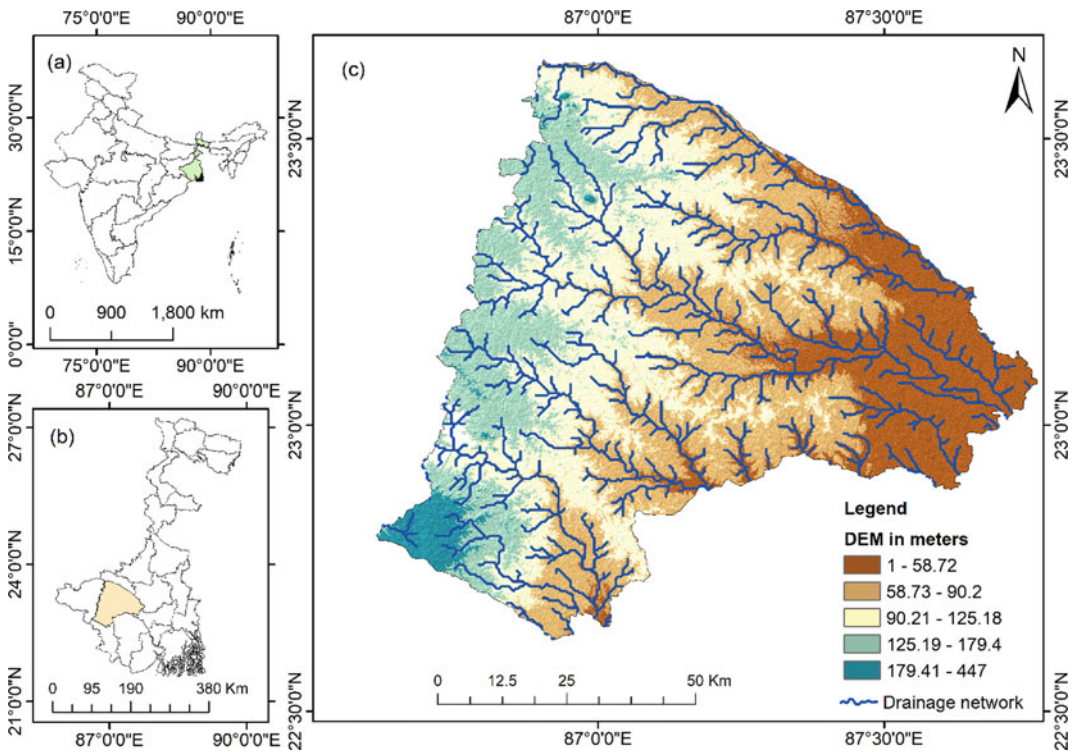


**Fig. 4.1** Location map of the study area; **a** India, **b** West Bengal, and **c** Bankura

Landsat 8, Landsat 9 OLI/TIRS collection 2, level 1 images (Path: 139, Row: 044) were used for NDVI, VCI, LST, TCI, and VHI indices, obtained from the USGS Earth explorer website (<https://earthexplorer.usgs.gov>). The land use/land cover maps were prepared from Sentinel 2 images downloaded from <https://scihub.copernicus.eu> using a training sample and the maximum likelihood method in a QGIS semi-automatic classification plugin (SCP).

### 4.3.2 Methods

#### 4.3.2.1 Normalized Difference Vegetation Index (NDVI)

The Normalized Difference Vegetation Index (NDVI) is a widely used remote sensing index to assess vegetation density and health. NDVI measures the difference between the reflectance of near-infrared (NIR) and visible red (VIS) light, which is correlated with the amount of vegetation present in an area (Glenn and Tabb 2019). NDVI can be used to monitor vegetation growth and health over time, detect changes in land use, and assess the impact of environmental factors on vegetation. It is commonly used in agriculture to assess crop health and yield potential and in forestry to monitor forest health and detect changes due to natural or man-made disturbances (Nejadrekabi et al. 2022).

Every geographical space has some carrying capacity (Kogan 1995). For estimating carrying capacity, we used NDVI. The maximum NDVI represents the highest carrying capacity, and the minimum NDVI represents a geographical area's lowest carrying capacity (ecosystem potential). NDVI also helps monitor crop yields, crop growth conditions, the health status of vegetation, and drought (Kogan 1995; Liu et al. 2021). The main concept of NDVI is that the healthy green leaves' internal mesophyll reflects near-infrared (NIR), whereas a large proportion of visible red radiation (VIS) is absorbed by leaf chlorophyll and other pigments. But in the case of water stress and unhealthy vegetation, the internal structure reacts reverse (Moisa et al. 2022).

$$NDVI = (NIR - RED)/(NIR + RED).$$

NDVI is calculated between the difference between near-infrared (NIR) and visible red bands of the electromagnetic spectrum. The index ranges from  $-1$  to  $+1$ , with values closer to  $+1$  indicating higher levels of healthy vegetation and values closer to  $-1$  indicating little to no vegetation. In tropical and temperate rain forests, the value of NDVI ranges between 0.6 to 0.8, and in barren rock, sand, or snow area, it is below 0.1 (Dutta et al. 2015). There are some noise problems in NDVI. Sensor degradation, satellite change, change of satellite orbital drift, cloud, and aerosol are the sources of error (Kogan 1995). These weather-related NDVI problems must be overcome, and thus why Kogan (1995) suggested the Vegetation Condition Index (VCI).

#### 4.3.2.2 Vegetation Condition Index (VCI)

The Vegetation Condition Index (VCI) is derived from remote sensing data developed for monitoring drought characteristics such as duration, intensity, spatial extent, and severity assessment. In this present chapter, VCI was used to monitor the Bankura district's agricultural drought by this equation.

$$VCI = (NDVI - NDVI_{MIN})/(NDVI_{MAX} - NDVI_{MIN}) * 100,$$

whereas NDVI,  $NDVI_{MIN}$ ,  $NDVI_{MAX}$  are multiyear maximum and minimum values of NDVI. According to Kogan (1995), the VCI value is measured in percentile ranges from 0 to 100. The classification of VCI is shown in Table 4.2. When the value is near 100, it defines favorable condition for crop, but the value 0 or near 0 indicate bad crop condition.

#### 4.3.2.3 Land Surface Temperature (LST)

Land surface temperature (LST) was calculated from the thermal infrared sensor (TIRS) band of Landsat 8 and 9 images from 2013 to 2022. The LST value ranges between 7500 and 65,535

**Table 4.2** Detailing the threshold value of VCI, TCI, and VHI

Range	Dryness level
0–10	Extreme drought
10–20	Severe drought
20–30	Moderate drought
30–40	Light drought
> 40	No drought

(Wan 2006), and it was reclosed by 0.02 to convert into Kelvin unit. It represents the radiative skin temperature of the land surface from solar radiation. In this chapter, LST was converted and rescaled into degree Celsius.

LST is gained by these equations.

$$\text{LST} = (\text{BT}/(1 + (\lambda * \text{BT}/\rho) * \text{Ln}(\varepsilon))) - 273.15,$$

where LST = Land surface temperature in Celsius (°C).

BT = Sensor brightness temperature in (°C).

$\lambda$  = Wavelength of thermal band of various Landsat satellite.

$\varepsilon$  = Emissivity of the land surface.

$\rho = (h \times (c/\sigma))$ , which is equal to  $1.438 \times 10^{-2}$  mK.

In which,  $\sigma$  is the Boltzmann constant ( $1.380649 \times 10^{-23}$  J/K),  $h$  is Plank's constant ( $6.62607015 \times 10^{-34}$  J.s), and  $c$  is the velocity of light ( $3 \times 10^8$  m/s).

#### 4.3.2.4 Temperature Condition Index (TCI)

The Temperature Condition Index (TCI) is a remote sensing index that provides an estimation of the vegetation's response to temperature stress. It measures the deviation of land surface temperature (LST) from its long-term average value and is based on the assumption that vegetation is sensitive to temperature anomalies (Swain et al. 2011). TCI is obtained by this equation.

$$\text{TCI} = (\text{LST}_{\text{MAX}} - \text{LST})/(\text{LST} - \text{LST}_{\text{MIN}}) * 100,$$

where LST is the value of the land surface temperature of a particular month, and  $\text{LST}_{\text{MAX}}$  and  $\text{LST}_{\text{MIN}}$  is the temperature of the studying period. LST provides information about the vegetation of the area. If LST increases, then the evapotranspiration of plants also increases, and surface soil moisture also reduces, which is a good indicator of vegetation stress (Kogan 1995; Seiler et al. 1998). The TCI value ranges between 0 and 100. A high value of TCI indicates a favorable condition for a crop, whereas a low value of TCI indicates an adverse effect on vegetation or drought conditions.

#### 4.3.2.5 Vegetation Health Index (VHI)

Vegetation Health Index (VHI) is the outcome of the combination of products extracted from vegetation signals, namely NDVI. It combines VCI and TCI (Orlovsky et al. 2011).

$$\text{VHI} = a \times \text{VCI} + (1 - a) \times \text{TCI},$$

where VHI represents the vegetation health index,  $a = 0.5$  similar contribution of VCI and TCI, VCI is the vegetation condition index, and TCI is the temperature condition index.

## 4.4 Results and Discussion

### 4.4.1 Land Use and Land Cover (LULC) Changes

The supervised classification with maximum algorithm method was employed to prepare land use and land cover (LULC) maps using Sentinel 2 images in the QGIS SCP plugin (Patil et al.

2012). The maps were categorized into six major types, including water body, vegetation cover, agricultural land, build-up area, bare ground, and range land, for the years 2018, 2019, 2020, 2021, and 2022, as depicted in Fig. 4.2 and Table 4.3.

The areal coverage or extension and areal changes from 2018 to 2022 have been detected through ArcGIS software, and it has been summarized in (Table 4.3). The LULC classification in 2018 (Fig. 4.2a) depicts that the majority of the area in Bankura district was under agricultural land (64.28%), the rest 18.24, 8.04, 2.72, and 1.10% areas are under vegetation cover, range land, build-up area, water body, and bare ground, respectively. Similarly, in 2019, the greatest share of land was occupied by also agricultural land (64.21%), and the trend of occupancy remained the same, i.e., land under vegetation cover (18.53%), range land (8.04%), build-up area (5.62%), water body (2.72%), and bare ground (1.02%) individually. Considering the trend of extension and rate (in %) of changes of each LULC from 2018 to 2022, vegetation cover and build-up areas increased by 3.90%,

partly in Barjora, Sonamukhi, Taldangra, Onda, Vishnupur, Ranibundh blocks of this district and 27.21% in some parts of blocks like Indus, Kotalpur, Patrasayar, Jaypur, Vishnupur, Bankura I sequentially, whereas percentage of land occupancy in bare ground, range of land, and water body decreased by  $-32.555$  and  $-19.75\%$  partly in Mejhia, Gangajalghati, Chhatna, and  $-9.84\%$  at Ranibundh and Hirbundh blocks in the same period. Taking into consideration the overall study period, vegetation cover and build-up areas have shown their areal increment. In contrast, water bodies, agricultural land, bare ground, and range land have harshly diminished in the same period due to many unscientific activities like unplanned settlement, massive grazing, and resultant soil degradation. Unlike build-up areas and vegetation cover, the land share of water bodies, agricultural land, bare ground, and range land has been increased. It is also a remarkable point that build-up areas has increased in a far larger percentage than vegetation cover, proving that most of the bare ground, range land, water body, and agricultural land are

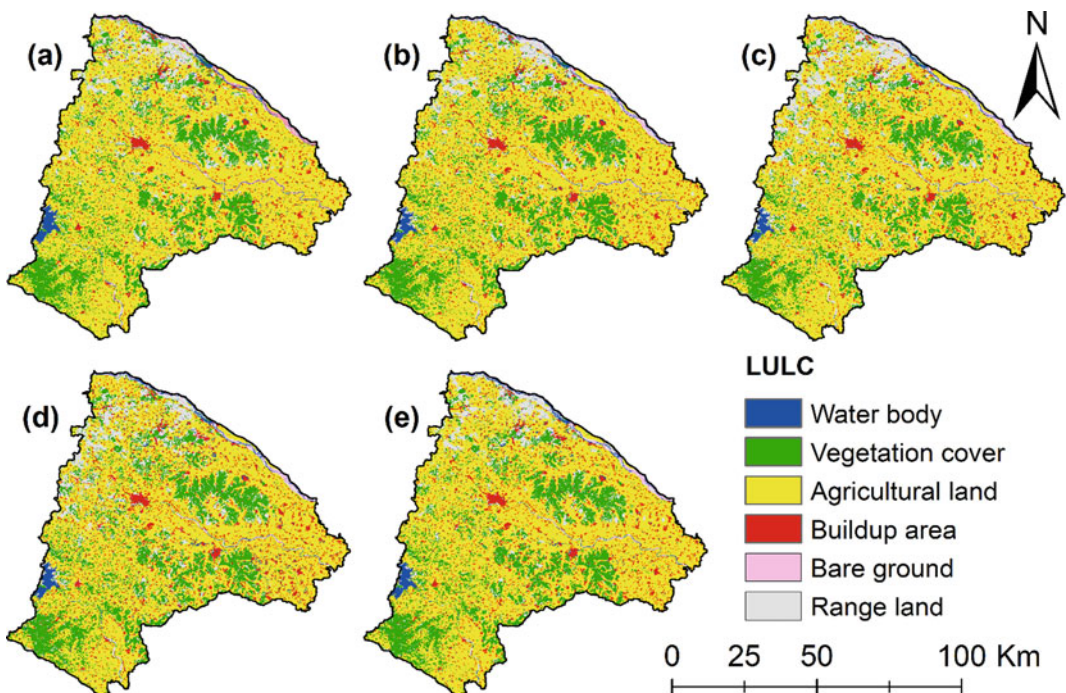


**Fig. 4.2** Land use and land cover (LULC); **a** 2018, **b** 2019, **c** 2020, **d** 2021, and **e** 2022

**Table 4.3** Land use and land cover (LULC) extent and change detection between 2018 and 2022

Sl No	Land use	2018	2019	2020	2021	2022	% of change
1	Water body	2.72	2.36	1.98	2.72	2.45	- 9.84
2	Vegetation cover	18.24	18.53	17.22	19.64	18.95	3.90
3	Agricultural land	64.28	64.21	63.04	59.82	64.25	- 0.04
4	Build-up area	5.62	6.71	6.86	7.88	7.15	27.21
5	Bare ground	1.10	1.02	0.91	0.79	0.74	- 32.55
6	Range land	8.04	7.17	10.00	9.16	6.46	- 19.75

converted to build-up areas but rationally maintains the vegetation-covered area by not unscientifically destruction of trees and continue the afforestation program. Considering the overall study period, the pattern of land use changes demonstrates that land occupancy of water body was increased from 2018 to 2019, then decreased in 2020, and again increased in 2021, but a little bit decreased in 2022. Land share of vegetation cover increased from 2018 to 2019, then decreased and continue to increase in 2021 which decreased in 2022. Agricultural land area decreased from 2018 to 2019, 2020, and 2021 but increased in 2022. In the build-up area, the land occupancy increased from 2018 to 2021 but decreased in 2022. The area under bare and range land has gradually reduced from 2018 to 2019, and so on. Generally, the result has revealed that a series of LULC changes in the study area for five years (2018–2022) shows the fact that build-up areas are most dominating in this area, indicating the continuous increment of human residence by maintaining green areas, whereas other land use pattern shows declining nature.

#### 4.4.2 Normalized Difference Vegetation Index (NDVI)

It measures the photosynthetic activities of vegetation by indicating favorable vegetation conditions with high value and unfavorable vegetation conditions associated with low NDVI value (Cunha et al 2015). Five principal changes

in vegetation (significant vegetation loss, vegetation loss, no vegetation change, vegetation gain, significant vegetation gain) have been detected from 2013 to 2022. Significant vegetation loss, which accounts for 5.42% of the total area, has been partially detected from 2013 to 2022 in Barjora, Sonamukhi, Patrasayar, Indus, Vishnupur, Sarenga, Raipur, Khatra blocks. The most worrying fact is that 48.17% vegetation loss in Mejhia, Gangajalpati, Barjora, Sonamukhi, Patrasayar, and Indus in the northeastern part of Bankura District, Bankura I and II, Onda in the middle part and Ranibundh, Raipur, Serenga in the southern part of this district is registered due to different unscientific construction work. In the meantime, about 12.64% area of the southwestern part is marked as an unchanged vegetation-covered area. Interestingly, 33.45% area has gained vegetation, whereas only 0.32% area has gained significant vegetation (Fig. 4.3 and Table 4.4).

This chapter has monitored the agricultural drought of the Bankura district from the year 2013 to 2022 by using the VCI technique. Figure 4.4 and Table 4.5 depict area-wise extreme, severe, moderate, and no drought conditions for ten years. Meanwhile, 79.65% (most of the area) area of this district was under extreme drought conditions in 2017 due to erratic rainfall and the low water-holding capacity of the soil. Community development blocks like Indus, Kotulpur, Jaypur, and Serenga accounted for extreme drought in 2014, 2015, and 2018. The maximum area (14.37%) under severe drought was in 2014,

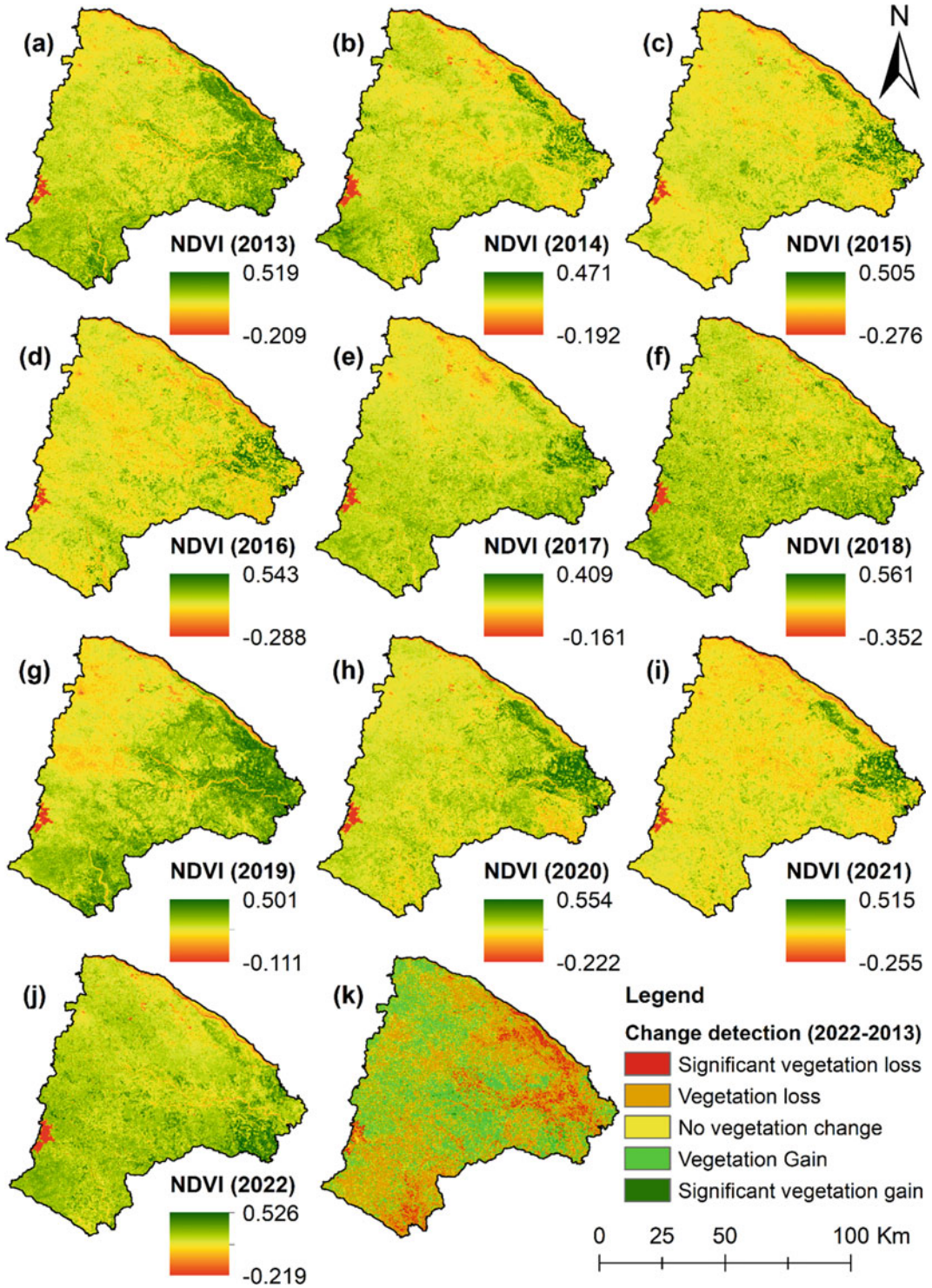


**Fig. 4.3** Normalized Difference Vegetation Index (NDVI); a 2013, b 2014, c 2015, d, 2016, e 2017, f 2018, g 2019, h 2020, i 2021, j 2022, and k Change detection



**Table 4.4** Vegetation change detection between 2013 and 2022

Sl. No	Level	Area in sq km	Area in %
1	Significant vegetation loss	373.75	5.42
2	Vegetation loss	3319.68	48.17
3	No vegetation change	871.00	12.64
4	Vegetation gain	2305.29	33.45
5	Significant vegetation gain	21.79	0.32

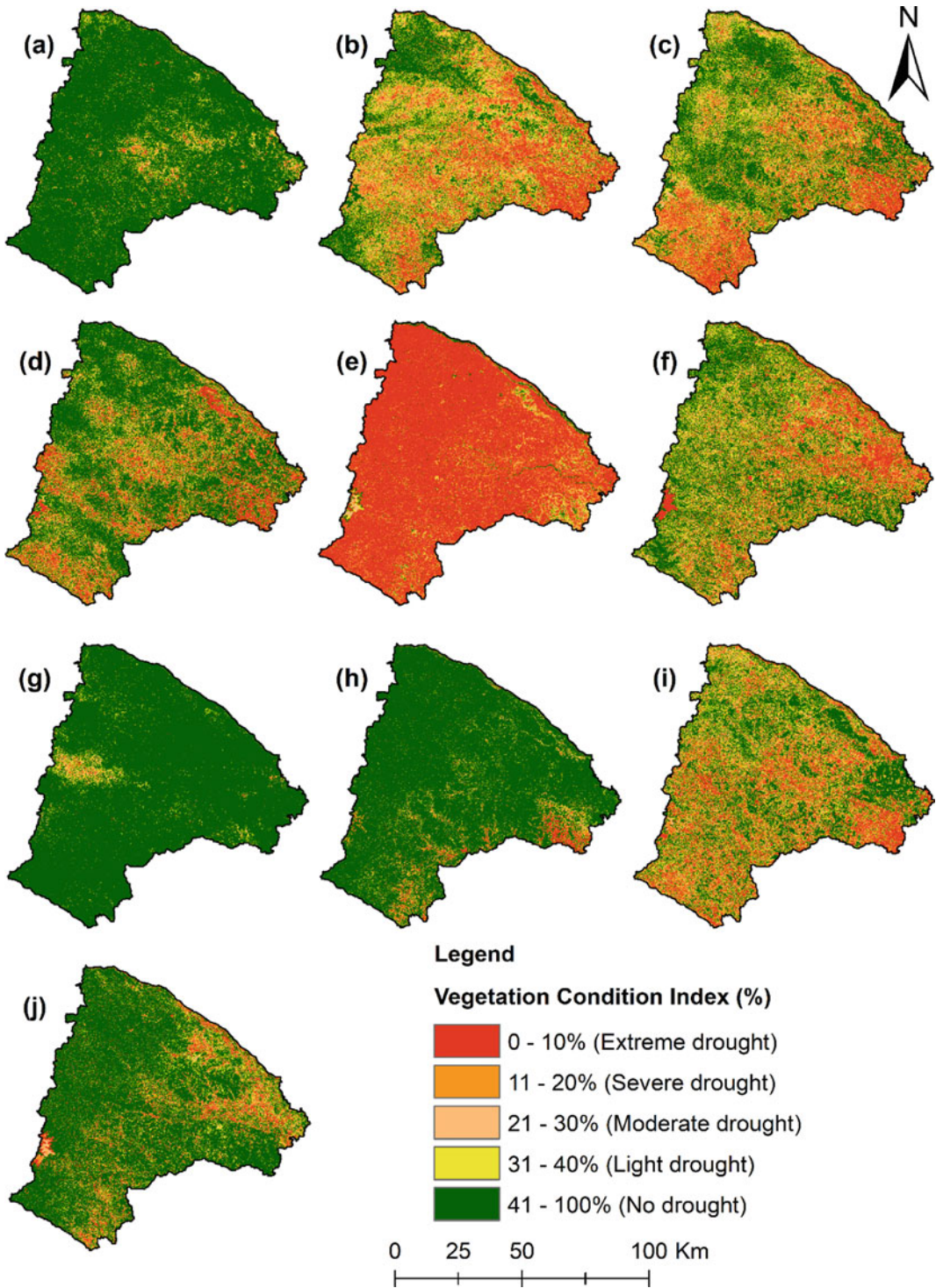
whereas 18.58 and 18.24% areas of the total were affected by moderate and light drought, respectively, in 2014, and a large area (95.50%) was registered as no drought-affected area in 2019 due to a sufficient amount of rainfall.

Figure 4.5 and Table 4.6 have assessed descriptive statistics (minimum, maximum, and mean temperature in °C) and standard deviation by considering ten years from 2013 to 2022 with the association of the LST technique. It illustrates that the lowest minimum temperature was recorded as 4.95 °C in 2014 and 25.40 °C in 2019. On the other hand, the maximum land surface temperature was 53.83 °C in 2018 and 35.43 °C in 2014. Low land surface temperature indicates dense vegetation cover and a low infiltration rate with minimum soil moisture, whereas high land surface temperature reveals no or thin vegetation cover with a high infiltration rate and maximum soil moisture. The highest mean temperature was recorded as 34.13 in 2016, and the lowest was 22.46 in 2014, respectively. The highest SD was recorded as 3.65 in 2014 and 1.79 in 2019, respectively. Their mean value shows the average fluctuation of temperature throughout ten years by calculating the average value for each year separately, whereas standard deviation shows the consistency among the distribution of mean temperature delicately.

In this chapter, TCI was calculated from Landsat 8, 9, and TIRS band 10 to categorize agricultural drought in five categories, i.e.,

extreme, severe, moderate, light, and no drought for the above said ten years. In 2016, 7.92% area of Bankura district was under extreme drought, the intensity of which reduced through rest years and remarkably in 2017 to 0.01%. While community development blocks like Chattna, Bankura I, and II, Taldangra, Simlapal, Khatra, Ranibundh, etc., were affected. On the other hand, 32.33% of the area in 2015 was identified as a severely drought-affected area, the areal extent of which was lowered to 0.01% in 2014. 29.65% area, including Chattna, Indpur, Bankura I, and Onda blocks, were under moderate drought-affected areas. 25.98 and 0.05% areas were recognized as the highest and lowest light drought-prone areas, respectively. 99.89% area of the Bankura district was not faced with drought in 2014, but it was reduced to 2.39% in 2017 (Fig. 4.6 and Table 4.7).

VHI, a combined indicator of vegetation health, depicts spatio-temporal drought variation in the Bankura district from 2013 to 2022 and is classified into five types. Figure 4.7 and Table 4.8 demonstrate that 18.96% area, including Chattna, Bankura I, Onda, and Ranibudh blocks, was extremely drought in 2016. This condition improved in 2014 by showing a 0.02% area under this adverse condition. The severe drought area was 27.92% in 2018 and gradually reduced to 0.04% in 2014. This fact clearly shows the improvement of drought conditions by applying canal irrigation, drilling irrigation, submersible



**Fig. 4.4** Drought monitoring using Vegetation Condition Index (VCI); a 2013, b 2014, c 2015, d 2016, e 2017, f 2018, g 2019, h 2020, i 2021, and j 2022

**Table 4.5** Spatio-temporal drought variation using Vegetation Condition Index (VCI)

Year	Extreme drought		Severe drought		Moderate drought		Light drought		No drought	
	Area		Area		Area		Area		Area	
	Sq. km	(%)	Sq. km	(%)	Sq. km	(%)	Sq. km	(%)	Sq. km	(%)
2013	55.51	0.81	90.77	1.32	198.65	2.88	356.79	5.18	6189.79	89.82
2014	1249.24	18.13	990.33	14.37	1280.26	18.58	1257.33	18.24	2114.34	30.68
2015	1075.03	15.60	920.88	13.36	1058.05	15.35	1128.15	16.37	2709.39	39.31
2016	833.95	12.10	631.40	9.16	712.77	10.34	777.86	11.29	3935.53	57.11
2017	5489.40	79.65	628.74	9.12	380.27	5.52	201.14	2.92	191.96	2.79
2018	1028.42	14.92	748.81	10.87	1070.95	15.54	1207.80	17.53	2835.52	41.15
2019	16.42	0.24	36.16	0.52	88.92	1.29	168.66	2.45	6581.36	95.50
2020	146.08	2.12	173.31	2.51	203.32	2.95	246.33	3.57	6122.48	88.84
2021	1086.36	15.76	980.26	14.22	1097.40	15.92	1034.36	15.01	2693.13	39.08
2022	427.40	6.20	344.26	5.00	466.24	6.77	611.26	8.87	5042.35	73.17

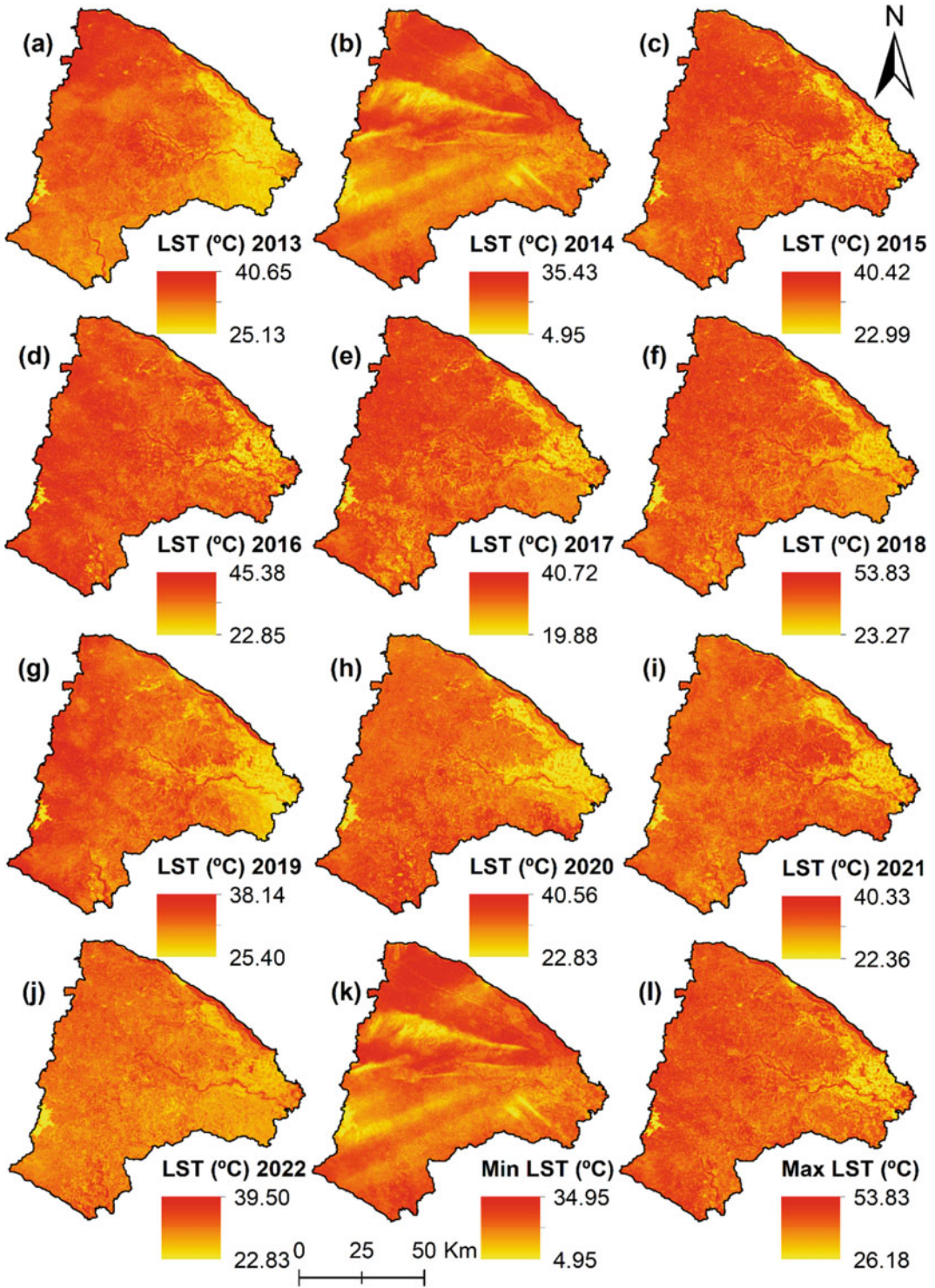


**Fig. 4.5** Land surface temperature (LST); a 2013, b 2014, c 2015, d 2016, e 2017, f 2018, g 2019, h 2020, i 2021, j 2022, k minimum temperature, and l maximum temperature

**Table 4.6** Descriptive statistics of land surface temperature from 2013 to 2022

Year	Minimum	Maximum	Mean	SD
2013	25.13	40.65	31.56	2.26
2014	4.95	35.43	22.46	3.65
2015	22.99	40.42	32.34	2.37
2016	22.85	45.38	34.13	2.78
2017	19.88	40.72	28.44	2.08
2018	23.27	53.83	33.36	2.88
2019	25.40	38.14	31.44	1.79
2020	22.83	40.56	29.84	2.22
2021	22.36	40.33	31.34	2.22
2022	22.84	39.50	29.19	1.83

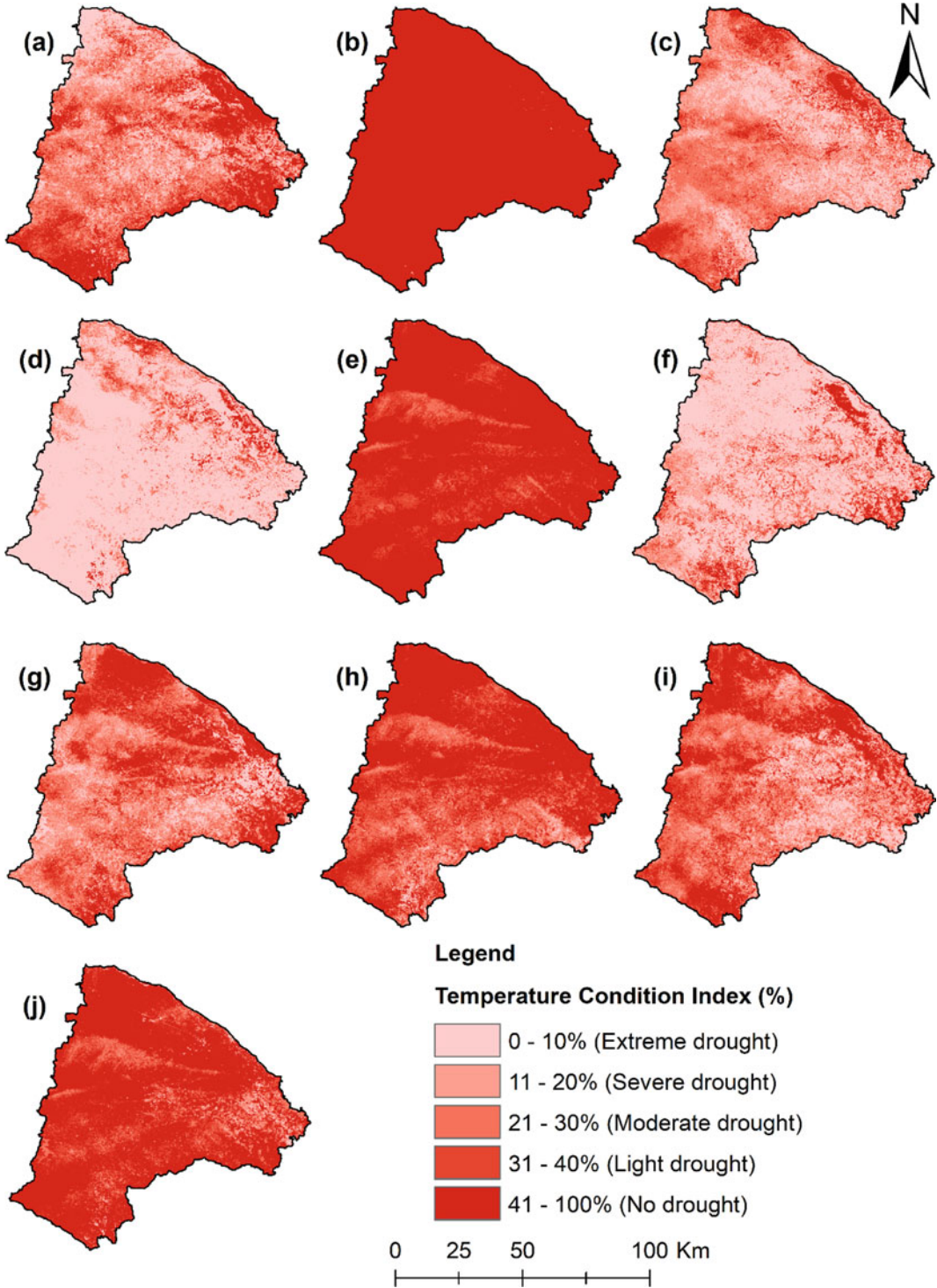


**Fig. 4.6** Drought monitoring using Temperature Condition Index (TCD); **a** 2013, **b** 2014, **c** 2015, **d** 2016, **e** 2017, **f** 2018, **g** 2019, **h** 2020, **i** 2021, and **j** 2022

**Table 4.7** Spatio-temporal drought variation using temperature condition index (TCI)

Year	Extreme drought		Severe drought		Moderate drought		Light drought		No drought	
	Area		Area		Area		Area		Area	
	Sq. km	(%)	Sq. km	(%)	Sq. km	(%)	Sq. km	(%)	Sq. km	(%)
2013	1070.19	15.53	1629.41	23.64	1749.54	25.39	1137.66	16.51	1304.71	18.93
2014	1.06	0.02	0.91	0.01	1.83	0.03	3.48	0.05	6884.23	99.89
2015	1363.97	19.79	2228.30	32.33	2043.04	29.65	783.74	11.37	472.47	6.86
2016	5232.01	75.92	881.13	12.79	428.21	6.21	185.25	2.69	164.90	2.39
2017	0.86	0.01	4.25	0.06	201.21	2.92	1208.40	17.53	5476.80	79.47
2018	4031.84	58.50	1462.82	21.23	699.42	10.15	317.08	4.60	380.35	5.52
2019	634.80	9.21	1515.30	21.99	1932.91	28.05	1315.07	19.08	1493.43	21.67
2020	97.43	1.41	359.93	5.22	1352.10	19.62	1790.62	25.98	3291.43	47.76
2021	709.47	10.29	1382.04	20.05	1906.45	27.66	1417.24	20.57	1476.30	21.42
2022	64.33	0.93	175.87	2.55	619.79	8.99	1502.11	21.80	4529.42	65.72

irrigation, etc. While, 39.73% area in 2017, including partly Indpur, Onda, Vishnupur, Tal-dangra, Khatra, Simlapal, the northern part of Ranibundh, Raipur blocks were recognized as the highest percentage of moderate drought-affected area and reduced at 0.16% in 2014. 24.84% area and was accounted for light drought-affected area in 2017. Most areas in this district faced no drought in 2014, which (positively) increased substantial water sources for agriculture.

## 4.5 Conclusion

In conclusion, the study presents a comprehensive analysis of spatio-temporal agricultural drought monitoring using remote sensing indices in Bankura district of West Bengal. The results show that severe drought conditions have affected various parts of the study area, leading to the abandonment of agricultural lands due to water and soil moisture scarcity. The study identifies specific areas that require urgent attention,

including Chattna, Bankura I, Onda, Ranibudh, Indus, Kotulpur, Jaypur, and Serenga blocks, where water shortage is a significant concern for sustainable agricultural practices. The findings suggest that strengthening water resource infrastructure, adopting agricultural water-saving technologies, and promoting seasonal rainwater harvesting could mitigate the impacts of drought in the region. Moreover, the study recommends the implementation of sustainable drought policies, including alteration of sowing and planting times, preservation agriculture, and zero tillage, modification of agricultural practices, to improve resilience toward the effects of drought. The study's results could inform policymakers, farmers, and other stakeholders in addressing local and regional drought issues, and prospective researchers could use them to advance knowledge in the field. Overall, the study provides valuable insights into the spatio-temporal dynamics of agricultural droughts and underscores the need for a comprehensive approach toward managing drought risks.

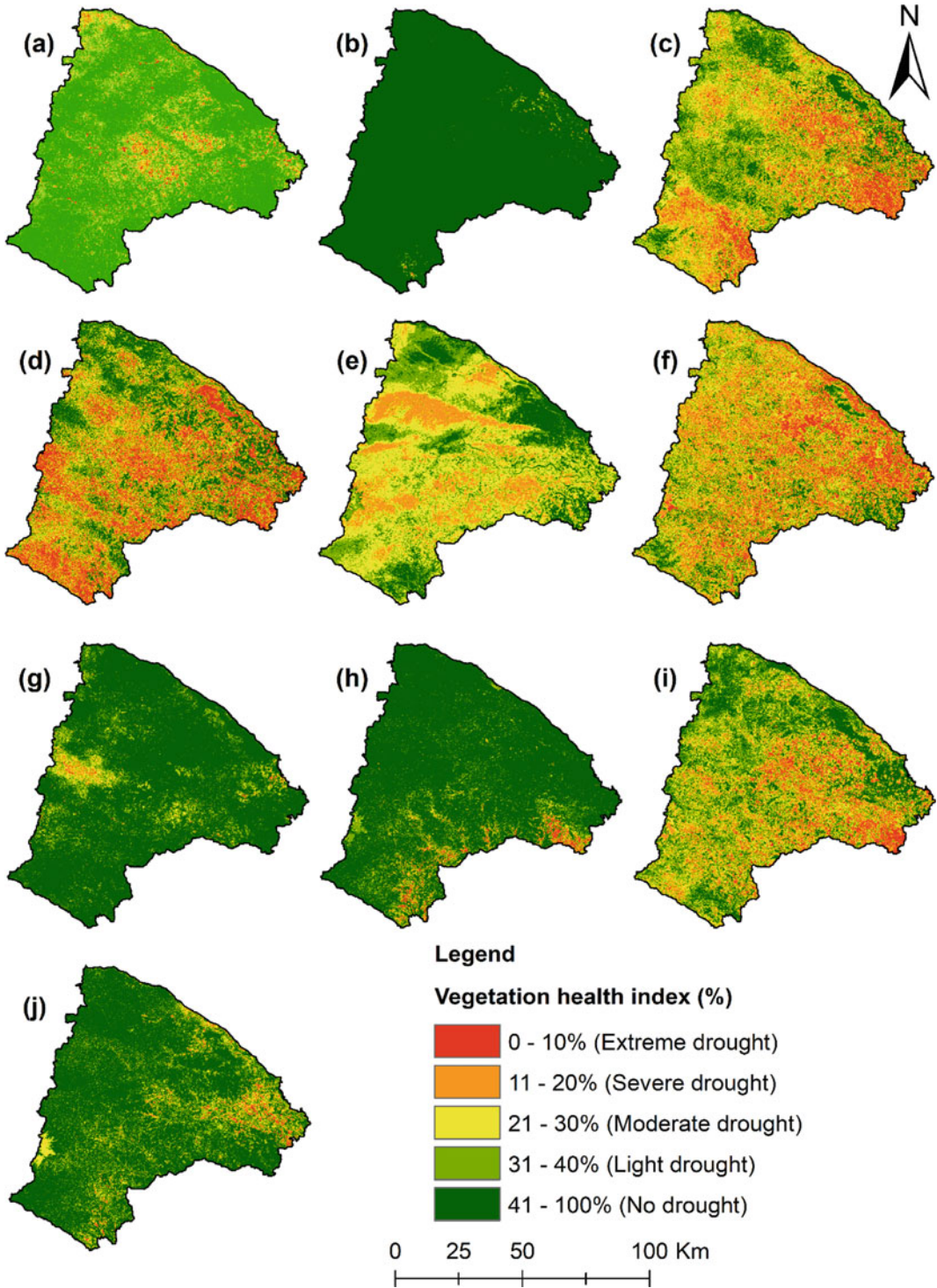


**Fig. 4.7** Drought monitoring using Vegetation Health Index (VHI) a 2013, b 2014, c 2015, d 2016, e 2017, f 2018, g 2019, h 2020, i 2021 and j 2022



**Table 4.8** Spatio-temporal drought variation using Vegetation Health Index (VHI)

Year	Extreme drought		Severe drought		Moderate drought		Light drought		No drought	
	Area		Area		Area		Area		Area	
	Sq. km	(%)	Sq. km	(%)	Sq. km	(%)	Sq. km	(%)	Sq. km	(%)
2013	51.87	0.75	201.21	2.92	556.18	8.07	1104.93	16.03	4977.32	72.22
2014	1.62	0.02	2.96	0.04	10.77	0.16	33.51	0.49	6842.65	99.29
2015	690.57	10.02	1477.71	21.44	1916.88	27.82	1570.98	22.80	1235.37	17.93
2016	1306.43	18.96	1382.12	20.06	1430.71	20.76	1186.07	17.21	1586.17	23.02
2017	3.73	0.05	1167.35	16.94	2737.72	39.73	1711.64	24.84	1271.07	18.44
2018	1051.92	15.26	1923.97	27.92	1922.39	27.90	1078.19	15.65	915.04	13.28
2019	13.90	0.20	72.76	1.06	256.25	3.72	674.78	9.79	5873.82	85.23
2020	68.91	1.00	153.92	2.23	252.58	3.67	454.08	6.59	5962.02	86.51
2021	447.32	6.49	1153.87	16.74	1681.43	24.40	1605.22	23.29	2003.67	29.07
2022	59.99	0.87	202.81	2.94	527.86	7.66	855.45	12.41	5245.41	76.11

## References

- Alahacoon N, Edirisinghe M, Ranagalage M (2021) Satellite-based meteorological and agricultural drought monitoring for agricultural sustainability in Sri Lanka. *Sustainability* 13(6):3427. <https://doi.org/10.3390/su13063427>
- Alam J, Saha P, Mitra R, Das J (2023) Investigation of spatio-temporal variability of meteorological drought in the Luni River Basin, Rajasthan, India. *Arab J Geosci* 16(3):201. <https://doi.org/10.1007/s12517-023-11290-8>
- Apurv T, Cai X (2021) Regional drought risk in the contiguous United States. *Geophys Res Lett* 48(5):e2020GL092200-1–e2020GL092200-12. <https://doi.org/10.1029/2020GL092200>
- Ayugi B, Eresanya EO, Onyango AO, Ogou FK, Okoro EC, Okoye CO, Ongoma V et al (2022) Review of meteorological drought in Africa: historical trends, impacts, mitigation measures, and prospects. *Pure Appl Geophys* 179(4):1365–1386
- Basak A, Rahman ATMS, Das J, Hosonod T, Kisi O (2022) Drought forecasting using the Prophet Model in semi-arid climate region of western India. *Hydrol Sci J* 67(9):1397–1417. <https://doi.org/10.1080/02626667.2022.2082876>
- Bhunia P, Das P, Maiti R (2020) Meteorological drought study through SPI in three drought prone districts of West Bengal, India. *Earth Syst Environ* 4(1):43–55. <https://doi.org/10.1007/s41748-019-00137-6>
- Census of India (2011) District census handbook, Bankura, Government of India
- Cunha APM, Alvalá RC, Nobre CA, Carvalho MA (2015) Monitoring vegetative drought dynamics in the Brazilian semiarid region. *Agric for Meteorol* 214–215:494–505
- Das S, Choudhury MR, Nanda S (2013) Geospatial assessment of agricultural drought (a case study of Bankura District, West Bengal). *Int J Agric Sci Res (IJASR)* 3(2):1–27
- Das J, Gayen A, Saha P, Bhattacharya SK (2020) Meteorological drought analysis using Standardized Precipitation Index over Luni River Basin in Rajasthan, India. *SN Appl Sci* 2(9):1–17. <https://doi.org/10.1007/s42452-020-03321-w>
- Dutta D, Kundu A, Patel NR, Saha SK, Siddiqui AR (2015) Assessment of agricultural drought in Rajasthan (India) using remote sensing derived Vegetation Condition Index (VCI) and Standardized Precipitation Index (SPI). *Egypt J Remote Sens Space Sci* 18(1):53–63. <https://doi.org/10.1016/j.ejrs.2015.03.006>
- Gidey E, Dikinya O, Sebege R, Segosebe E, Zenebe A (2018) Analysis of the long-term agricultural drought onset, cessation, duration, frequency, severity and spatial extent using Vegetation Health Index (VHI) in Raya and its environs, Northern Ethiopia. *Environ Syst Res* 7(1):1–18
- Glenn DM, Tabb A (2019) Evaluation of five methods to measure normalized difference vegetation index (NDVI) in apple and citrus. *Int J Fruit Sci* 19(2):191–210
- Guo H, Wang R, Garfin GM, Zhang A, Lin D (2021) Rice drought risk assessment under climate change: based on physical vulnerability a quantitative assessment method. *Sci Total Environ* 751:141481. <https://doi.org/10.1016/j.scitotenv.2020.141481>
- Hadri A, Saidi MEM, Boudhar A (2021) Multiscale drought monitoring and comparison using remote sensing in a Mediterranean arid region: a case study from west-central Morocco. *Arab J Geosci* 14(2):1–18. <https://doi.org/10.1007/s12517-021-06493-w>

- Hoque M, Pradhan B, Ahmed N, Alamri A (2021a) Drought vulnerability assessment using geospatial techniques in Southern Queensland, Australia. *Sensors* 21(20):6896. <https://doi.org/10.3390/s21206896>
- Hoque MAA, Pradhan B, Ahmed N, Sohel MSI (2021b) Agricultural drought risk assessment of Northern New South Wales, Australia using geospatial techniques. *Sci Total Environ* 756:143600. <https://doi.org/10.1016/j.scitotenv.2020.143600>
- Kim JE, Yu J, Ryu JH, Lee JH, Kim TW (2021) Assessment of regional drought vulnerability and risk using principal component analysis and a Gaussian mixture model. *Nat Hazards* 109(1):707–724. <https://doi.org/10.1007/s11069-021-04854-y>
- Kogan FN (1995) Application of vegetation index and brightness temperature for drought detection. *Adv Space Res* 15(11):91–100. [https://doi.org/10.1016/0273-1177\(95\)00079-T](https://doi.org/10.1016/0273-1177(95)00079-T)
- Kogan FN (1997) Global drought watch from space. *Bull Am Meteor Soc* 78(4):621–636
- Liu Q, Zhang J, Zhang H, Yao F, Bai Y, Zhang S, Liu Q (2021) Evaluating the performance of eight drought indices for capturing soil moisture dynamics in various vegetation regions over China. *Sci Total Environ* 789:147803. <https://doi.org/10.1016/j.scitotenv.2021.147803>
- Moisa MB, Merga BB, Gemedo DO (2022) Multiple indices-based assessment of agricultural drought: a case study in Gilgel Gibe Sub-basin, Southern Ethiopia. *Theor Appl Climatol* 148(1):455–464. <https://doi.org/10.1007/s00704-022-03962-4>
- Nath R, Nath D, Li Q, Chen W, Cui X (2017) Impact of drought on agriculture in the Indo-Gangetic Plain, India. *Adv Atmos Sci* 34(3):335–346
- Nejadrekabi M, Eslamian S, Zareian MJ (2022) Spatial statistics techniques for SPEI and NDVI drought indices: a case study of Khuzestan Province. *Int J Environ Sci Technol* 19:6573–6594
- Orlovsky L, Kogan F, Eshed E, Dugarjav C (2011) Monitoring droughts and pastures productivity in Mongolia using NOAA-AVHRR data. In: *Use of satellite and in-situ data to improve sustainability*. Springer, Dordrecht, pp 69–79
- Patil MB, Desai CG, Umrikar BN (2012) Image classification tool for land use/land cover analysis: a comparative study of maximum likelihood and minimum distance method. *Int J Geol Earth Environ Sci* 2(3):189–196
- Pei F, Wu C, Liu X, Li X, Yang K, Zhou Y, Wang K, Xu L, Xia G (2018) Monitoring the vegetation activity in China using vegetation health indices. *Agric for Meteorol* 248:215–227
- Peng Y, Gitelson AA (2011) Application of chlorophyll-related vegetation indices for remote estimation of maize productivity. *Agric For Meteorol* 151(9):1267–1276. <https://doi.org/10.1016/j.agrformet.2011.05.005>
- Raha S, Gayen SK (2020) Simulation of meteorological drought using exponential smoothing models: a study on Bankura District, West Bengal, India. *SN Appl Sci* 2(5):909
- Seiler RA, Kogan F, Sullivan J (1998) AVHRR-based vegetation and temperature condition indices for drought detection in Argentina. *Adv Space Res* 21(3):481–484
- Sultana MS, Gazi MY, Mia MB (2021) Multiple indices based agricultural drought assessment in the north-western part of Bangladesh using geospatial techniques. *Environ Challenges* 4:100120-1–100120-17
- Swain S, Wardlow BD, Narumalani S, Tadesse T, Callahan K (2011) Assessment of vegetation response to drought in Nebraska using Terra-MODIS land surface temperature and normalized difference vegetation index. *Gisci Remote Sens* 48(3):432–455
- Wan Z (2006) MODIS land surface temperature products users' guide. Institute for Computational Earth System Science, University of California, SantaBarbara
- Wang JL, Yu YH (2021) Comprehensive drought monitoring in Yunnan Province, China using multisource remote sensing data. *J Mt Sci* 18(6):1537–1549. <https://doi.org/10.1007/s11629-020-6333-7>
- Zambrano F, Lillo-Saavedra M, Verbist K, Lagos O (2016) Sixteen years of agricultural drought assessment of the BioBio region in Chile using a 250 m resolution Vegetation Condition Index (VCI). *Remote Sens* 8(6):530
- Zeng J, Zhang R, Qu Y, Bento VA, Zhou T, Lin Y, Wang Q (2022) Improving the drought monitoring capability of VHI at the global scale via ensemble indices for various vegetation types from 2001 to 2018. *Weather Clim Extremes* 35:100412. <https://doi.org/10.1016/j.wace.2022.100412>
- Zhang B, Wu P, Zhao X, Wang Y, Gao X, Cao X (2013) A drought hazard assessment index based on the VIC-PDSI model and its application on the Loess Plateau, China. *Theor Appl Climatol* 114(1):125–138. <https://doi.org/10.1007/s00704-012-0826-4>
- Zhao X, Xia H, Liu B, Jiao W (2022) Spatiotemporal comparison of drought in Shaanxi–Gansu–Ningxia from 2003 to 2020 using various drought indices in Google Earth Engine. *Remote Sens* 14(7):1570. <https://doi.org/10.3390/rs14071570>